J. of Thermal Science Vol.12, No.1

Three Dimensional Separation with Spiral-Focus in a Decelerating Duct Flow (Effect of Asymmetric Inlet Boundary Layer Thickness)

Yoichi Kinoue Toshiaki Setoguchi Kenji Kaneko Mamun Mohammad
Department of Mechanical Engineering, Saga University, 1, Honjo, Saga, 840-8502, Japan
Masahiro Inoue
Department of Mechanical Engineering Science, Kyushu University, 6-10-1, Hakozaki, Higashi-ku, Fukuoka, 812-8581, Japan

An experimental apparatus was developed to study the three dimensional separated flow with spiral-foci. The internal decelerating flow was generated by the air suction from a side wall to produce the separation on an opposite-side wall. The relation between the upstream boundary layer and the generation of spiral-foci in the separation region was observed by a tuft method. As a result, it was clarified that the spiral-focus type separation could be produced on the side wall and its behavior was closely related to the vortices supplied into the separation region from the boundary layer developing along top wall or bottom one.

Keywords: three dimensional separation, spiral-focus, decelerating duct flow.

Introduction

The internal decelerating flow in rotor and stator cascades of axial fluid machines is fully complex three dimensional flow owing to the annular wall boundary layer developing along the hub and casing wall and the tip leakage flow. Especially under a condition of high blade loading or quite low flow rate, the three dimensional separated flow with a spiral-focus (or simply a focus) occurs because of large adverse pressure gradient[1~3]. Lucke and Gallus[2] showed that the spiral-focus was observed in the hub corner stall region by the oil flow visualization and the calculated limiting streamlines. Hah and Loellbach[3] showed that a single twister-like vortex whose two-legs originated from two distinct spiral-foci generated on the hub wall in stator by their numerical simulation. The generation of spiral-focus is considered to influence the blade loading of axial fluid machines because the generation of spiral-focus means the branching of bound vortex on the blade and is associated with the energy loss of cascades.

Other researches about the three dimensional separated flow can be seen in the area of aeronautics. Tobak and Peake[4,5] examined a three dimensional flow around a body such as a delta wing in view of the configuration of singular points (node, focus and saddle) and explained some experimental examples using mathematical topological formulas.

The purpose of this research is to clarify the fluid dynamics of three dimensional separated flow with spiral-focus at the internal decelerating flow generated by a suction from side wall in a wind tunnel which has square-shaped cross section. In this paper the apparatus, which was intended that the suction from side wall was uniform in space as a simple condition case, was used to examine the relation between the boundary layer developing along the top and bottom wall upstream of the suction part and the generation of spiral-focus in the three dimensional separated flow.

Experimental Apparatus and Procedure

The experimental apparatus is shown in Fig.1. It consists of an inlet contraction ② with an air filter ①, a rectangular duct with a test section ③, two suction ducts, an air collection chamber ⑨, and a centrifugal fan ⑩. One of the suction ducts is connected to a porous wall ⑤downstream of the duct to produce a mainstream at the test section, and another is connected to a porous side wall ④ of the test section to generate decelerating

Received 2002

flow. Air suction of both ducts is made by the centrifugal fan through the collection chamber with a bypass valve ⑨. Each suction duct has a flow nozzle ⑥ and a valve ⑦ to control the decelerating ratio.

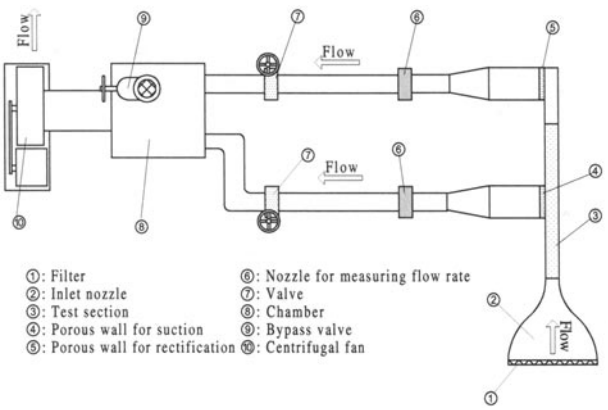

Fig. 1 Experimental apparatus

The test section is shown in Fig.2. It is made of transparent acrylic resin except the porous wall. Its cross section is 120 mm square and the length is 240 mm in the mainstream direction. The porous wall has 1152 holes arranged at grid points at equal intervals. The *xyz* coordinate system is adopted as shown in Fig.2. The *x*, *y* and *z* directions are defined as the mainstream, width and height direction, respectively. The porous wall is located from x=0 to x=240 mm. The velocity component of each direction is defined as *u*, *v* and *w*, respectively. A side wall opposite to the porous wall can be exchanged both for visualization and for static pressure measurement.

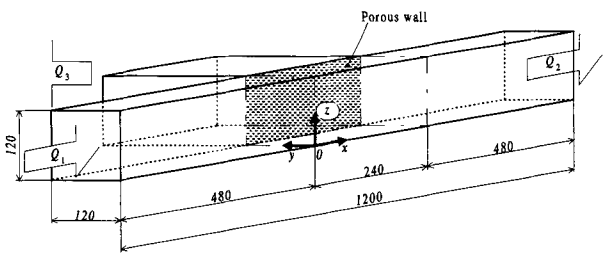

Fig. 2 Test section

In the present experiments, the inlet flow rate Q_1 was kept constant, so that the inlet mainstream velocity u_1 at the test section was 20 m/s. The outlet flow rate Q_2 at test section and the suction flow rate Q_3 were changed by controlling the valve ⑩ and a valve in the chamber ⑧. A Pitot-tube located at the center of the inlet test section was used for setting the flow rate Q_1. The flow nozzles were used for setting the flow rate Q_2 and Q_3.

Time-averaged wall static pressure on the smooth side wall (y=0) opposite to the porous wall was measured by using pressure taps and a pressure transducer with slow time response. The velocity profile in the test section and downstream of the porous side wall were measured by using a Pitot-tube. The flow fields near the bottom wall and the side wall were observed by a surface tuft method for flow visualization and recorded by using a digital CCD video camera. Silk threads of 15 mm in length were used as tuft and arranged at grid points at equal intervals of 10 mm. They were glued so as to keep tuft root perpendicular to wall.

In order to examine the effect of upstream boundary layer thickness on the separation, blocks of acrylic resin were equipped uniformly on the bottom wall in the area from x = –345 mm to –125 mm. The size of each block is 24 ✕ 24 mm and 5 mm-height. They were arranged in the checkerboard shape.

Experimental Results and Discussions

Velocity profiles

To make the air suction uniform from the porous wall, a preliminary experiment was carried out by changing porosity of the porous wall. Fig.3 shows the velocity profile measured by using Pitot-tube downstream of the porous wall in the suction duct for Q_3/Q_1 = 0.6 ((4) in Fig.1). The measuring location in Fig.3 is at y =180 mm and at z = 60 mm in the coordinate system shown in Fig.2. Although the velocity profiles are not flat in the case without porous plate (porosity of 100%) and in the cases of small value porosity of 7.1% and 12.6%, the comparatively flat profile is obtained by the porosity of 19.6%. Therefore, the porous wall with 19.6% porosity was used in the following experiment. It has 1152 holes with 2.5 mm-dia arranged at grid points at equal intervals of 5 mm.

Figs.4 and 5 show the velocity profiles in the *z*

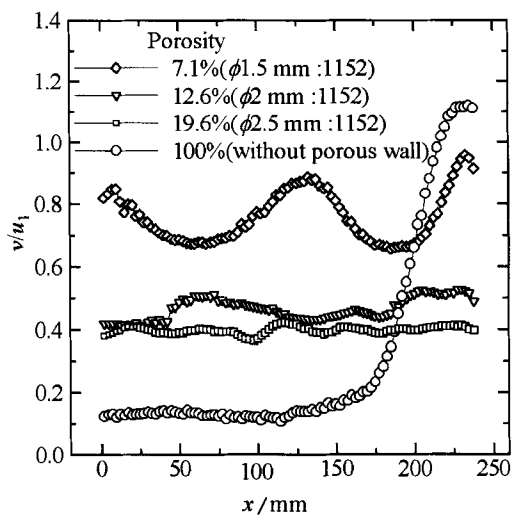

Fig. 3 Velocity profile downstream of the porous wall with Q_3/Q_1 = 0.6

direction at x=-60 mm for Q_3/Q_1 = 0 in the case of smooth upstream surfaces and of rough bottom surface upstream of the test section. In Fig.4, the velocity profile is almost symmetric to the centerline of the z direction for the smooth wall. On the other hand, in Fig.5, the velocity from z = 0 mm to 40 mm is lower than that in Fig.4, which means that the boundary layer along bottom wall become thicker owing to rough bottom wall.

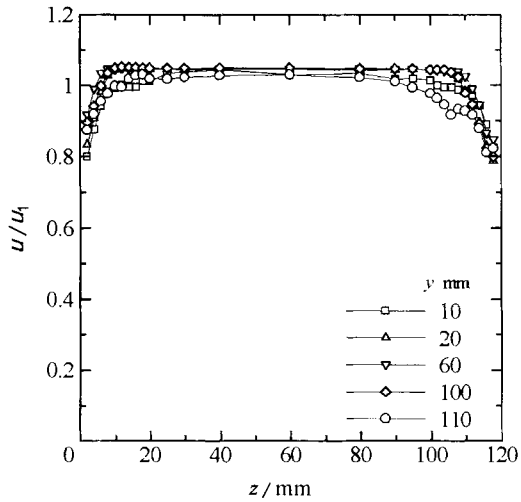

Fig. 4 Velocity profile upstream of test section with Q_3/Q_1=0.0 for smooth wall

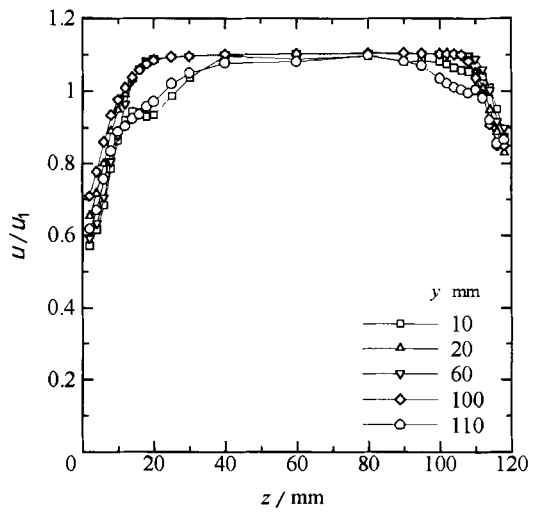

Fig. 5 Velocity profile upstream of test section with Q_3/Q_1 = 0.0 for rough bottom wall

Pressure coefficient profiles

Fig.6 shows the static pressure coefficient C_p on the side wall (y=0) opposite to the porous wall at z = 60 mm (in the center of height direction), where the wall static pressure is time-averaged and normalized by the dynamic pressure of the inlet flow. All the cases except for Q_3/Q_1=0, the static pressure profiles have adverse pressure gradient, which increases with increasing the ratio of flow rate Q_3/Q_1 in the upstream half of the test section (suction part). But the static pressure profile tends to be flat in a certain region of suction for Q_3/Q_1= 0.6, 0.8 and 1.0. These regions are considered to be separation region. The start point of separation moves toward upstream with increasing the ratio of flow rate Q_3/Q_1.

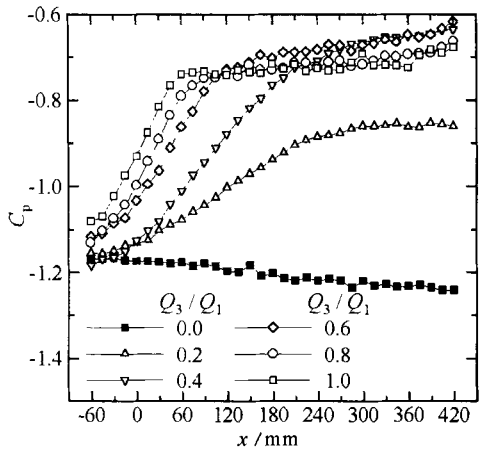

Fig. 6 Static pressure coefficient on the side wall at z=200mm for smooth wall

Figs.7 and 8 show the static pressure coefficient profiles on the side wall opposite to porous wall for Q_3/Q_1=0.8 in the cases of the smooth upstream surfaces and the rough upstream surface on the bottom wall, respectively. In Fig.7, difference in the profiles is so small in the z direction that the pressure field is considered to be two dimensional. In Fig.8, the pressure profiles for rough bottom wall show that the separation region appears more upstream at small value of z than at

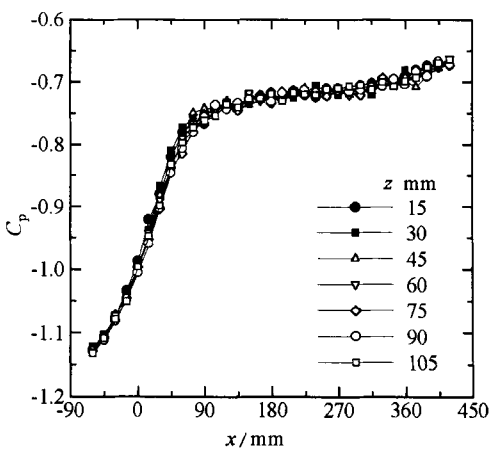

Fig. 7 Static pressure coefficient on the side wall with Q_3/Q_1=0.8 for smooth wall

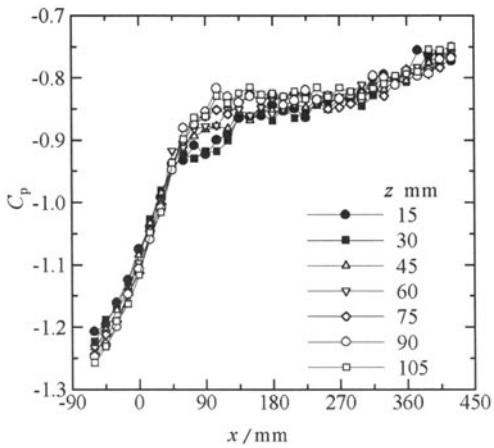

Fig. 8 Static pressure coefficient on the side wall with Q_3/Q_1=0.8 for rough bottom wall

large value of z, and the pressure field is three dimensional in the region of x=50~130 mm.

Flow visualization near the bottom wall

Figs.9 and 10 show the photographs of the flow near the bottom wall visualized by using the surface tuft method. The air flows from left to right. The porous wall is located at the top of each frame, and the lines between the the marks △ and ▽ indicate the start and end points of suction.

Figs.9(a), (b) and (c) are the photographs for Q_3/Q_1=0.6, 0.8 and 1.0 in the cases of smooth upstream

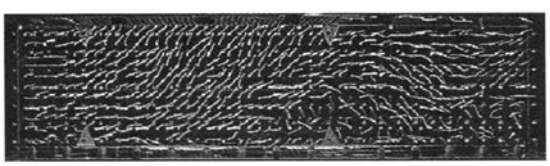

(a) $Q_3/Q_1 = 0.6$

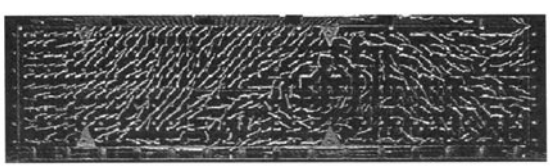

(b) $Q_3/Q_1 = 0.8$

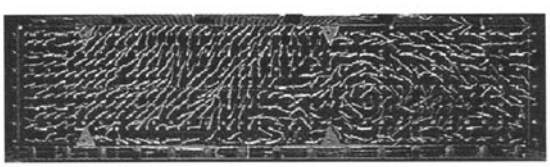

(c) $Q_3/Q_1 = 1.0$

Fig. 9 Flow visualization near the bottom wall for smooth wall

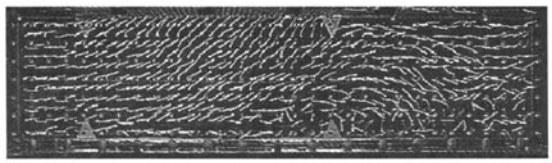

(a) $Q_3/Q_1 = 0.6$

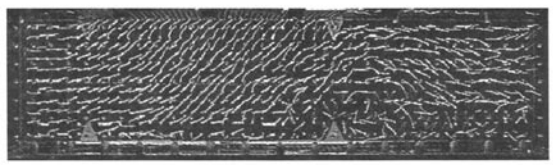

(b) $Q_3/Q_1 = 0.8$

(c) $Q_3/Q_1 = 1.0$

Fig. 10 Flow visualization near the bottom wall for rough bottom wall

surfaces. The area where the tuft directions tilt at random is considered to be separation region, and a clockwise vortex can be observed in each photograph in the separation region. Figs.10(a), (b) and (c) are the photographs showing the flow near the bottom wall for Q_3/Q_1 = 0.6, 0.8 and 1.0 in the cases of rough bottom wall. Larger separation region are observed in Fig.10 compared with Fig.9. Similar to Fig.9, a clockwise vortex can be observed in the separation region in each photograph of Fig.10. These vortices should be two-dimensional in the z direction if the two-dimensional flow can be generated ideally.

Flow visualization near the side wall

Figs.11 and 12 show the photographs of the flow near the side wall opposite to the porous wall visualized by using the surface tuft method. Again the flow comes from left to right and the lines between the marks △ and ▽ indicate the start or end points of suction.

Fig.11 is the photographs for Q_3/Q_1 = 0.6, 0.8 and 1.0 in the case of smooth upstream surface. Although the thickness of the upstream boundary layers on the top and bottom wall are nearly the same as shown in Fig.4, the separation line on the side wall is inclined considerably. In Figs.11(a), (b) and (c), the photographs indicate the flow patterns at the moment that the flow near bottom separates more upstream than the flow near top, whereas Figs.11(d), (e) and (f) show the flow patterns at the moment that the flow near top separates more upstream

than the flow near bottom. These two patterns were observed in turn at irregular intervals. A clockwise vortex is observed in the separation region in Figs.11 (a), (b) and (c), and a counterclockwise vortex is observed in the separation region in Figs.11(d), (e) and (f). The separated flow is considered to be three dimensional and a spiral focus can be observed at each moment, even if the time-averaged side wall pressure profile seems two dimensional in the height direction.

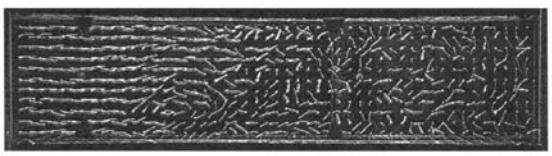

(a) $Q_3/Q_1 = 0.6$, from downside

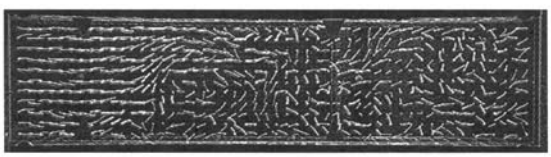

(b) $Q_3/Q_1 = 0.8$, from downside

(c) $Q_3/Q_1 = 1.0$, from downside

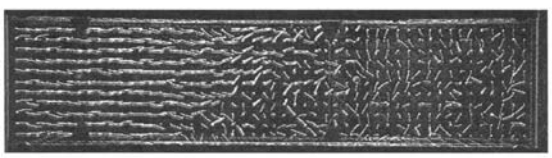

(d) $Q_3/Q_1 = 0.6$, from upside

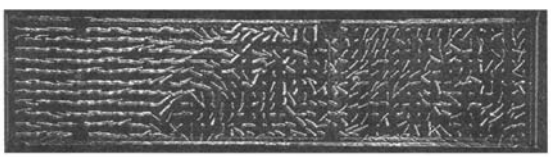

(e) $Q_3/Q_1 = 0.8$, from upside

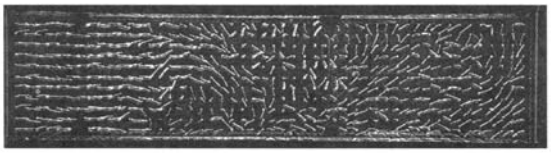

(f) $Q_3/Q_1 = 1.0$, from upside

Fig. 11 Flow visualization near the side wall for smooth wall

Figs.12(a), (b) and (c) show the photographs near the side wall opposite to the porous wall for $Q_3/Q_1 = 0.6$, 0.8 and 1.0 in the case of the rough bottom wall upstream of suction part. The flow near the bottom wall separates more upstream than the flow near the top wall. A clockwise vortex can be seen more clearly in the separation region than the case of smooth wall in Fig.11. Any counterclockwise vortex near the top wall can not be observed in this case.

The following discussion is made based on the above experimental results. In the boundary layer developing on the top wall upstream of the suction part counterclockwise vorticity is distributed, while clockwise vorticity is distributed on the bottom wall. In case that all the surfaces upstream of suction part are smooth, the counterclockwise and clockwise vorticities immigrate into the separation region from the top and bottom wall alternatively. It makes an alternate vortex at irregular intervals so that both of the vortices can be observed in the photographs as shown in Fig.11. On the other hand, in the case of rough bottom surface, the bottom wall boundary layer is thicker than the top wall. Much more clockwise vorticity is supplied from the bottom wall to the separation region than the counterclockwise vorticity from the top wall. Therefore only the clockwise vortices can be observed in the flow near the side wall. A spiral-focus generated on the side wall is considered to have close relation to the supplied vorticity from the top and bottom wall boundary layer developing upstream of the separation region.

(a) $Q_3/Q_1 = 0.6$

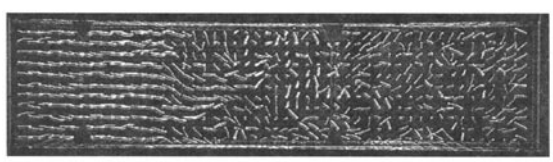

(b) $Q_3/Q_1 = 0.8$

(c) $Q_3/Q_1 = 1.0$

Fig.12 Flow visualization near the side wall for rough bottom wall

Conclusions

In order to study the fluid dynamics of three dimensional separated flow with spiral-focus at the internal decelerating flow, an experimental apparatus was developed in which the decelerating flow is generated by suction from side wall. The generation of spiral-focus in the separation region was observed by a tuft method by changing the boundary layer thickness on the upstream walls. The conclusions obtained are summarized as follows:

1. Uniform suction in space can be done by sucking air through the porous wall adjusted.

2. Time-averaged side wall static pressure is two dimensional and has little difference in the height direction in case that all the wall surfaces are smooth upstream of the test section.

3. In the case of smooth wall, two typical flow patterns appear alternatively at irregular intervals. One is the case that the flow near the bottom wall separates more upstream than the flow near the top wall and a clockwise vortex can be seen in the separation region. Another is the case that similar flow occurs near the top wall and a counterclockwise vortex can be seen in the separation region.

4. In the case of rough bottom wall upstream of the test section, only the first case can be seen and a clockwise vortex in the separation region can be seen more clearly than the case of the smooth wall.

5. A spiral-focus generated on the side wall is considered to have close relation to the vorticities supplied from the upstream boundary layer developing along the top and bottom wall.

References

[1]Inoue, M. Vortex and Turbomachinery. In: Proceedings of the 5th Asian International Conf. on Fluid Machinery. 1997, 1: 117—131

[2]Lucke, J R, Gallus, H E. Analysis of Separated Flows Inside an Annular Compressor Cascade Using a Low-*Re*-Number k-ε- and an Algebraic Reynolds-Stress-Model. ASME GT Paper, 1997, 97-GT-132

[3]Hah, C, Loellbach, J. Development of Hub Corner Stall and Its Influence on the Performance of Axial Compressor Blade Rows. ASME Journal Turbomachinery, 1999, 121: 67—77

[4]Tobak, M, Peake, D J. Topology of Two-Dimensional and Three-Dimensional Separated Flows. AIAA 12th Fluid and Plasma Dynamics Conference, 1979, AIAA-79-1480

[5]Tobak, M, Peake, D J. Topology of Three-Dimensional Separated Flows, Annual Review of Fluid Mechanics, 1982, 14: 61—85